J. Astrophys. Astr. (2018) 39:26
https://doi.org/10.1007/s12036-018-9515-8

Creating an isotopically similar Earth–Moon system with correct angular momentum from a giant impact

BRYANT M. WYATT[1,*], JONATHAN M. PETZ[1,2], WILLIAM J. SUMPTER[1,2], TY R. TURNER[1,2], EDWARD L. SMITH[1,2], BAYLOR G. FAIN[3], TAYLOR J. HUTYRA[1,3], SCOTT A. COOK[1], JOHN H. GRESHAM[1], MICHAEL F. HIBBS[3] and SHAUKAT N. GODERYA[3,4]

[1] Department of Mathematics, Tarleton State University, Stephenville, TX 76402, USA.
[2]Department of Engineering and Computer Science, Tarleton State University, Stephenville, TX 76402, USA.
[3]Department of Chemistry, Geoscience, and Physics, Tarleton State University, Stephenville, TX 76402, USA.
[4]Program for Astronomy Education and Research, Tarleton State University, Stephenville, TX 76402, USA.
*Corresponding author. E-mail: wyatt@tarleton.edu

MS received 20 October 2017; accepted 5 January 2018; published online 13 March 2018

Abstract. The giant impact hypothesis is the dominant theory explaining the formation of our Moon. However, the inability to produce an isotopically similar Earth–Moon system with correct angular momentum has cast a shadow on its validity. Computer-generated impacts have been successful in producing virtual systems that possess many of the observed physical properties. However, addressing the isotopic similarities between the Earth and Moon coupled with correct angular momentum has proven to be challenging. Equilibration and evection resonance have been proposed as means of reconciling the models. In the summer of 2013, the Royal Society called a meeting solely to discuss the formation of the Moon. In this meeting, evection resonance and equilibration were both questioned as viable means of removing the deficiencies from giant impact models. The main concerns were that models were multi-staged and too complex. We present here initial impact conditions that produce an isotopically similar Earth–Moon system with correct angular momentum. This is done in a single-staged simulation. The initial parameters are straightforward and the results evolve solely from the impact. This was accomplished by colliding two roughly half-Earth-sized impactors, rotating in approximately the same plane in a high-energy, off-centered impact, where both impactors spin into the collision.

Keywords. Accretion—Earth—Moon—planetary formation—planet-disk interaction.

1. Introduction

The canonical giant impact hypothesis (Hartmann & Davis 1975; Cameron and Ward 1976; Stevenson 1987) states that an impactor roughly the size of Mars obliquely struck proto-Earth. The dense iron cores of proto-Earth and the impactor merged to form Earth's core. A substantial amount of the outer silicate material was ejected into orbit around the newly formed Earth and coalesced into our Moon. Simulations of the canonical impact (Benz *et al.* 1986; Canup & Asphaug 2001; Canup 2004, 2008) yield correct angular momentum, but produce a circumplanetary disk of debris composed of a relatively large amount of material from the impactor (Meier 2012; Zhang *et al.* 2012). Detailed analysis of the Moon samples reveal striking isotopic similarities between the Earth and Moon (Lugmair & Shukolyukov 1998; Wiechert *et al.* 2001; Meier 2012; Zhang *et al.* 2012), making it unlikely that the Moon could be composed predominantly of impactor material (Stevenson 2014). Attempts have been made to reconcile this issue, but all have led to complex multi-stage models (Canup 2013).

Pahlevan and Stevenson (2007) proposed adding equilibration to the canonical model to resolve the isotopic concerns. Turbulent mixing between the Earth and the circumplanetary disk could have created a Moon that was isotopically similar to Earth. Other researchers modified the canonical impact to create models that would, from the impact, produce an Earth and a circumplanetary disk that were isotopically similar. This could be done in two ways: (i) create a disk that was composed

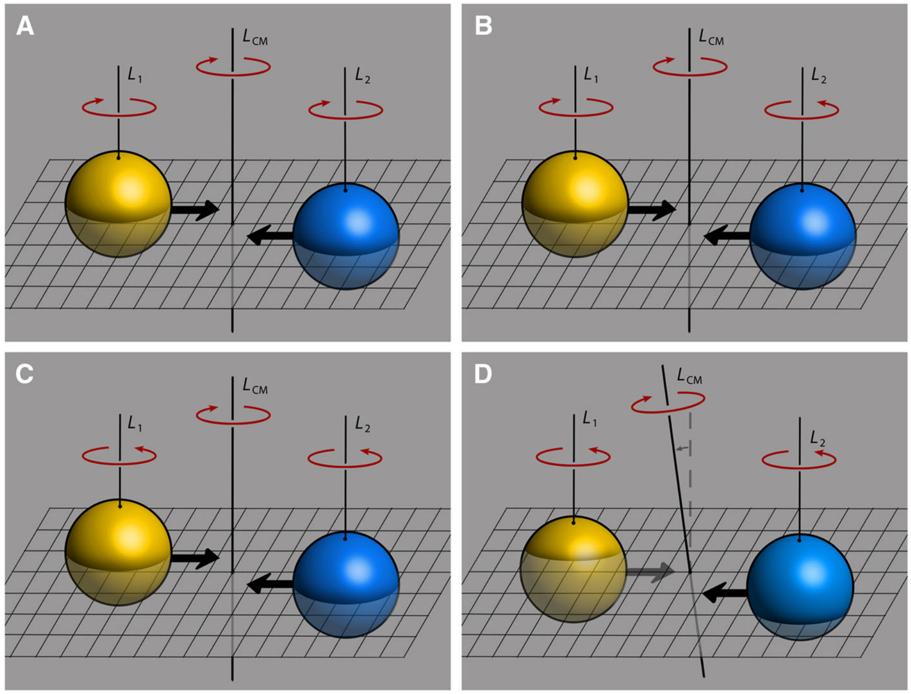

Figure 1. Collision scenarios. The black arrows represent the impactors' relative velocities. The red arrows represent the impactors' spins. Impactor 2 (blue) has an initial position towards the reader. In scenario d, the impactors' equatorial planes are parallel but separated.

predominantly of proto-Earth material, or (ii) produce an Earth and a disk that were both composed of relatively equal amounts of material from both impactor and target. Ćuk and Stewart (2012) used a small impactor colliding with a rapidly spinning proto-Earth to create a disk composed predominantly of material from the proto-Earth. Canup (2012) used impactors of equal size in an off-centered collision to create an Earth and disk composed of equal amounts of material from both impactors. Eiland *et al.* (2014) used impactors of equal size in an off-centered collision, coupled with impactor spins, to create an Earth and a Moon composed of equal parts from both impactors. Reufer *et al.* (2012) used a hit-and-run scenario that produced a disk composed predominantly of material from proto-Earth. These variations were successful in addressing the isotopic concerns, but all produced an Earth–Moon system with excess angular momentum. Ćuk and Stewart (2012) proposed using evection resonance between the Moon and the Sun as a mechanism to remove the excess angular momentum.

The Royal Society found these approaches lacking and called for new models (Canup 2013; Clery 2013; Elliott & Stewart 2013; Stevenson & Halliday 2014). Our goal in responding to the call was not to produce a new modeling method. The goal was to find initial conditions that would allow existing methods to produce simulations where isotopic similarity and correct angular momentum evolve naturally from the collision. Thus, we present a summary of our findings.

2. Methods

Consider the scenarios depicted in Fig. 1. There are three contributors to the angular momentum of the system: the spin of impactor 1, the spin of impactor 2, and the rotation of the entire system about its center of mass created by the off-centered impact. We denote them L_1, L_2, and L_{cm} respectively. An impactor is said to spin into the collision if its spin is opposed to L_{cm}, and out of the collision if its spin aligns with L_{cm}. Kinetic energy comes from impactor spins and the impact velocity.

Figure 1a shows a coplanar, off-centered collision, where both impactors spin out of the collision. This produced smooth and predictable results. By adjusting the spin rates, initial linear velocities, and the off-center displacement, the composition and size of the resulting Moon could be controlled. However, all runs that produced enough orbiting material to create the Moon suffered from excess angular momentum. The resultant angular momentum was roughly twice that of the measured value for the Earth–Moon system. Here, L_1, L_2, and L_{cm} augment each other, giving little latitude

Table 1. Initial values for impactors.

Parameter	Body 1 (yellow)	Body 2 (blue)
Center of mass	(− 44500, − 200, − 1810) km	(44500, 200, 1810) km
Linear velocity	(8.8, 0.0, 0.0) km/s	(− 8.8, 0.0, 0.0) km/s
Angular velocity	(0.0, 0.43, 0.0) rev/h	(0.0, 0.43, 0.0) rev/h
% of Earth's mass	55	55
% Iron by mass	26	26
% Silicate by mass	74	74
No. of compute-elements	65,536	65,536

to reduce angular momentum without reducing kinetic energy.

Figure 1b shows a coplanar, off-centered collision where impactor 2 spins into the collision and impactor 1 spins out of the collision. This allowed the reduction of angular momentum while keeping the kinetic energy of the system high, because L_2 was opposed to L_1 and L_{cm}. However, the released material was almost exclusively from the impactor spinning out of the collision. Hence, this type of impact did not satisfy the isotopic similarity condition.

Figure 1c shows a coplanar, off-centered collision where both impactors spin into the collision. This allowed easy reduction of angular momentum while keeping kinetic energy high, since both L_1 and L_2 were opposed to L_{cm}. The inward rotations limited lateral escape of material. If the kinetic energy was sufficiently high, the collision was violent and chaotic, and large amounts of material were ejected above and below the collision plane. This was a surprising result, because in all of our previous work with lunar-forming impacts, the majority of ejected material was released laterally along the collision plane. Due to the fact that the impact was coplanar and symmetric, most of the ejected material was released perpendicular to the collision plane with little lateral component to produce an orbit and returned straight back to Earth. This resulted in an insufficient amount of orbital debris. However, a positive result was that the debris was released and composed of equal amounts of material from both impactors.

Figure 1d shows a collision identical to Fig. 1c, except that the equatorial planes of the impactors are separated, which produced an additional contribution to angular momentum not seen in Fig. 1a–c. This additional angular momentum component tilted the axis along which material was primarily ejected, giving the ejected material an angular component which increased the amount of orbital debris. The orbital debris was massive enough to create the Moon, was iron-poor, and was composed of relatively equal amounts of material from both impactors. The angular momentum of the resulting system could also be controlled while keeping kinetic energy high. This type of impact satisfied all necessary conditions. An interesting observation (see section 4) about this type of collision is that the orbital plane of the ejected material is close to orthogonal to the equatorial plane of the newly formed Earth.

3. Results

If kinetic energy is high and the initial total angular momentum is chosen to be close to the observed value of the Earth–Moon system, the type of collision depicted in Fig. 1d consistently produced favorable results. To demonstrate the robustness of this type of collision, a simulation is presented where the initial impactor spins and velocities were selected from Ćuk and Stewart's (2012) paper. The remaining initial conditions were then chosen so that the angular momentum for the entire system would be close to what is measured for the Earth–Moon system today. Ćuk and Stewart (2012) present a series of runs where proto-Earth is spinning with a 2.3-hour rotational period and is hit with impactors whose ratio of impact velocity to mutual escape velocity (v_{imp}/v_{esc}) range from 1 to 3. In the simulation presented here, both impactors were given a 2.3-hour rotational period and an impact ratio v_{imp}/v_{esc} equal to 2. See Table 1 for a full list of initial conditions. In this simulation, the ejected material which formed the orbital debris was iron-free, and composed of 59.3% material from impactor 1 and 40.7% material from impactor 2. The resultant Earth was composed of 49.5% material from impactor 1, and 50.5% material from impactor 2. The angular momentum of the resultant Earth–Moon system was 3.5677×10^{28} (kg · km^2/s) which is only 2.7% off today's measured value of 3.4738×10^{28} (kg · km^2/s). The ratio of the size of

Table 2. Results 2464.48 hours into the simulation.

Parameter	Earth	Moon
Mass	6.3106×10^{24} kg	7.4551×10^{22} kg
Iron elements impactor1	8,479	0
Iron elements impactor2	8,478	0
Silicate elements impactor1	54,582	497
Silicate elements impactor2	53,457	1253
Ratio impactor1/impactor2	0.982	2.521
% Iron material by mass	27.1	0.0
% Silicate material by mass	72.9	100.0
Axial tilt off collision plane	15.83 degrees	

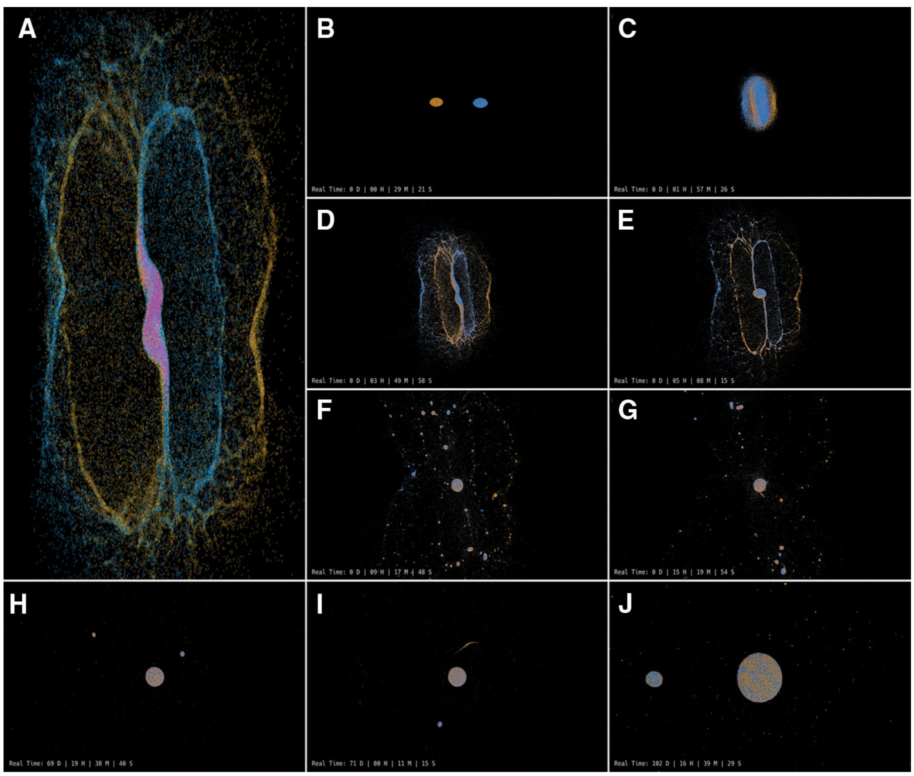

Figure 2. Inwardly rotating, off-planar, off-center collision. Impactor 1 (left, silicate-yellow, iron-red); impactor 2 (right, silicate-blue, iron-purple). The impactors have parallel equatorial planes. The planes are slightly offset, with plane 1 below plane 2. These side views shows the orthogonal release of material. (A) The apex of the collision with the iron elements enhanced. (B–G) Snap shots 0.49, 1.95, 3.82, 5.13, 9.28, and 15.32 hours into the collision. (H) Two dominant moons in orbit. (I) Destruction of the companion moon at 1704.18 hours. (J) Earth and Moon at 2464.48 hours at which time the statistics of the Earth–Moon system were gathered.

the Earth to that of the Moon was 84.65, which is only 4.1% off the actual ratio of 81.28. Additional results are presented in Table 2. The collision is illustrated in Fig. 2. Details of the simulation technique are presented in Appendix A. Videos of the simulation can be viewed at https://youtu.be/6IjA8FwhWp0 or obtained b contacting the corresponding author.

In summary, it was observed that if two roughly half-Earth-sized impactors, rotating in approximately the same plane, collide in a high-energy, off-centered impact — where both impactors spin into the collision — an iron-deficient Moon composed of large percentages of material from both impactors can form. In addition, the resulting Earth–Moon system can have an angular momentum comparable to what we see today. The collisions are violent, but this is in line with recent papers on high-energy impact and vigorous mixing during Moon-forming events (Wang & Jacoben 2016; Young *et al.* 2016). It may be unusual to have two large impactors collide at this stage of the evolution of our solar system, but our Moon is an unusual satellite.

4. Discussion

One interesting result of this type of collision is that the equatorial plane of the Earth and the average orbital plane of the ejected material are nearly orthogonal. The orbit of the ejected material is only slightly prograde to Earth's axial spin. This was initially surprising. However, the Moon's orbit today is substantially off the equatorial plane (Bradley 1748; Walker & Zahnle 1986). Tidal forces produced by Earth's rapid rotation are transferring energy to the Moon, causing it to move outward, parallel to the Earth's equatorial plane (Darwin 1879; Goldreich 1966; Touma & Wisdom 1994). This process is constantly reducing the angle between the Moon's orbit and the equatorial plane. Hence, the Moon's off-equatorial orbit is produced naturally with the initial conditions presented here, and will evolve toward what we see today. Though our approaches differ, this is a similar result reported in Ćuk *et al.*'s (2016) paper.

Another interesting result is that two dominant moons usually emerge and orbit the Earth for an extended period of time. On most occasions, one of the moons drives the other moon inside Earth's Roche limit where it is ripped apart by Earth's gravity. However, in rare cases, the two moons collide, which is in line with companion moon theories of the differences between the near and far side of the Moon (Jutzi & Asphaug 2011). It should be noted that this is an N-body simulation which tends to produce moons rapidly (Kokubo *et al.* 2000).

5. Conclusion

In conclusion, we believe that initial conditions of the type depicted in Fig. 1d will resolve the issues the Royal Society identified with the giant impact hypothesis. The method presented here is a modification of the canonical giant impact scenario, but is not a major deviation from the standard model like the multiple-impact model recently presented by Rufu *et al.* (2017). In addition, the initial conditions we present may help answer additional open questions about the Earth–Moon system. We hope others will utilize these initial conditions in their models to see if they produce similar results.

Acknowledgements

We thank NVIDIA and Mellanox Technologies for the donation of hardware; Tarleton State University's high-performance computing lab for space; Tarleton State University's Office of Research and Innovation, and The Program for Astronomy Education and Research for funding; Robert W. Muth for insightful remarks and suggestions; and special thanks to The Wyatt Fund for supporting student travel.

Appendix A. Methods

To perform an extensive search of the initial parameter space, we sought a simulation method that was computationally inexpensive and easily parallelized to run on modern graphics processing units. Eiland *et al.*'s (2014) method was ideal for this purpose because it adopts a simplified approach to thermodynamics, yet is otherwise physically realistic. Another advantage of Eiland's method is that it frequently produces a fully formed Moon, whereas other methods typically only produce a circumplanetary disk of debris. The parameter settings used with Eiland's method are listed in Table 3.

The simulation code was written in C, C++, and Compute Unified Device Architecture (CUDA). The simulations were run on workstations housing CUDA-enabled NVIDIA graphics processing units (GPUs). The graphics code was written in C and C++ and displayed using OpenGL. Gravity was not approximated; the full all-pairs n-body problem was used. This was numerically integrated through time using the leapfrog formulas.

The input parameters were: the number of computational-elements, mass of impactor 1, mass of impactor 2, iron/silicate ratio by mass of impactor 1, iron/silicate ratio by mass of impactor 2, density of iron material, and density of silicate material (see Table 1 and Table 3). Using these inputs, a common radius for all computational-elements was determined. The correct number of silicate and iron computational-elements was then designated to create each impactor.

Given the computational-elements assignments, we first randomly placed the iron computational-elements into two separate spheres that would become the cores of impactor 1 and impactor 2. The radii of these spheres were calculated by doubling the radii

Table 3. Parameters for Eiland's model.

Parameter	Value
D	290.46 km
M_{Si}	$4.2601 \cdot 10^{19}$ kg
M_{Fe}	$1.0073 \cdot 10^{20}$ kg
K_{Si}	1.5×10^{14}kg · km^{-1} · s^{-2}
K_{Fe}	1.5×10^{14}kg · km^{-1} · s^{-2}
KRP_{Si}	0.01
KRP_{Fe}	0.01
SDP_{Si}	0.002
SDP_{Fe}	0.02
epsilon	0.0 km
Time step	5.8717 s
Density Silicate material	3.32×10^{12}kg · km^{-3}
Density Iron material	7.85×10^{12}kg · km^{-3}

determined by a 68% packing ratio for their respective iron computational-elements. Next, the silicate computational-elements were placed to create the mantles of impactor 1 and impactor 2. These computational-elements were placed outside the core spheres but inside spheres whose radii were calculated by doubling the radii determined by a 68% packing ratio for the impactors' total computational-elements, respectively. If a computational-element was randomly placed less than a diameter from an existing computational-element, a new position was randomly selected until the computational-element was successfully placed.

The computational-elements positioned in these unnatural, randomly selected positions had high potential energy. This energy was removed by allowing the internal computational-elements of each impactor to interact under a large damping constraint for 20 simulated hours. This damping constraint was then removed and the impactors were again allowed to run for 50 simulated hours to remove any residual effects caused by the damping component. The impactors were then spun and allowed to settle into their spins for 50 simulated hours. During this building process, impactors were isolated from each other. The final step was to give impactors initial positions and velocities. All computational-elements were then allowed to interact, starting the simulation. Positions and velocities were periodically stored to create videos and to gather statistics.

References

Benz, W., Slattery, W. L., Cameron, A. G. W. 1986, Icarus 66, 515

Bradley, J. 1748, Philos. Trans. R. Soc. London 45, 1

Cameron, A. G. W., Ward, W. R. 1976, Proc. Lunar Planet. Sci. Conf. 7, 120–122

Canup, R. M. 2004, Icarus 168, 433–456

Canup, R. M. 2008, Icarus 196, 518–538

Canup, R. M. 2012, Science 338, 1052–1055

Canup, R. M. 2013, Nature 504, 27–29

Canup, R. M., Asphaug, E. 2001, Nature 412, 708–712

Clery, D. 2013, Science 342, 183–185

Ćuk, M., Hamilton, D. P., Lock, S. J., Stewart, S. T. 2016, Nature 539, 402–406

Ćuk, M., Stewart, S. T. 2012, Science 338, 1047–1052

Darwin, G. H. 1879, Philos. Trans. R. Soc. London 170, 447–538

Eiland, J. C., Salzillo, T. C., Hokr, B. H., Highland, J. L., Mayfield, W. D., Wyatt, B. M. 2014, J. Astrophys. Astr. 35, 607–618

Elliott, T., Stewart, S. T. 2013, Nature 504, 90–91

Goldreich, P. 1966, Rev. Geophys. 4, 411–439

Hartmann, W. K., Davis, D. R. 1975, Icarus 24, 504–515

Jutzi, M., Asphaug, E. 2011, Nature 496, 69–71

Kokubo, E., Ida, S., Makino, J. 2000, Icarus 148, 419–436

Lugmair, G. W., Shukolyukov, A. 1998, Geochim. Cosmochim. Acta 62, 2863–2886

Meier, M. M. M. 2012, Nat. Geosci 5, 240–241

Pahlevan, K., Stevenson, D. J. 2007, Earth Planet. Sci. Lett. 262, 438–449

Reufer, A., Meier, M. M. M., Benz, W., Wieler, R. 2012, Icarus 221, 296–299

Rufu, R., Aharonson, O., Perets, B. H. 2017, Nature Geoscience 10, 89–94

Stevenson, D. J. 1987, Ann. Rev. Earth Planet. Sci. 15, 271–300

Stevenson, D. J. 2014, Physics Today 67, 32–38

Stevenson, D. J., Halliday, A. N. 2014, Phil. Tran. R. Soc. A 372, 1–3

Touma, J., Wisdom, J. 1994, Astron. J. 108, 1943–1961

Walker, J. C. G., Zahnle, K. J. 1986, Nature 320, 600–602

Wang, K., Jacoben, S. B. 2016, Nature 538, 487–490

Wiechert, U., Halliday, A. N., Lee, D. C., Snyder, G. A., Taylor, L. A., Rumble, D. 2001, Science 294, 345–348

Young, E. D., Kohl, I. E., Warren, P. H., Rubie, D. C., Jacobson, S. A., Morbidelli, A. 2016, Science 351, 493–496

Zhang, J., Dauphas, N., Davis, A. M., Leya, I., Fedkin, A. 2012, Nat. Geosci 5, 251–255